Composite Interfaces, Vol. 15, No. 5, pp. 495–514 (2008)

Also available online - www.brill.nl/ci

Microdeformation behaviour of Al–SiC metal matrix composites

D. P. MYRIOUNIS [1,2], S. T. HASAN [2] and T. E. MATIKAS [1,*]

[1] *University of Ioannina, Department of Materials Science and Engineering, University Campus, 45110 Ioannina, Greece*
[2] *Sheffield Hallam University, Materials and Engineering Research Institute, City Campus, S1 1WB, Sheffield, UK*

Received 2 July 2007; accepted 19 October 2007

Abstract—The satisfactory performance of metal matrix composites depends critically on their integrity, the heart of which is the quality of the matrix-reinforcement interface. The nature of the interface depends in turn on the processing of the MMC component. At the micro-level, the development of local concentration gradients around the reinforcement can be very different according to the nominal conditions. These concentration gradients are due to the metal matrix attempting to deform during processing. This plays a crucial role in the micro-structural events of segregation and precipitation at the matrix-reinforcement interface. Equilibrium segregation occurs as a result of impurity atoms relaxing in disordered sites found at interfaces, such as grain boundaries, whereas non-equilibrium segregation arises because of imbalances in point defect concentrations set up around interfaces during non-equilibrium heat treatment processing. The amount and width of segregation depend very much on (a) the heat treatment temperature and the cooling rate, (b) the concentration of solute atoms and (c) the binding energy between solute atoms and vacancies. An aluminium–silicon–magnesium alloy matrix reinforced with varying amounts of silicon carbide particles was used in this study. A method of calculation has been applied to predict the interfacial fracture strength of aluminium, in the presence of magnesium segregation at metal matrix interface. Preliminary results show that the model succeeds in predicting the trends in relation to segregation and intergranular fracture strength behaviour in these materials. Microhardness profiles of reinforced and un-reinforced aluminium alloys are reported. The presence of precipitates at alloy-reinforcement interface identified by Nano-SEM.

Keywords: Particulate reinforced aluminium alloys; metal matrix composites; interfacial strength; deformation; precipitation.

*To whom correspondence should be addressed. E-mail: matikas@otenet.gr

1. INTRODUCTION

Aluminium MMCs have great promise for high temperature, high strength and wear resistant applications. Aluminium alloys are important materials in many industrial applications, including aerospace. Silicon carbide particulate reinforced aluminium metal matrix composites, which are especially attractive due to their superior strength, stiffness, low cycle fatigue properties, corrosion fatigue behaviour, creep resistance and wear resistance compared with the corresponding wrought aluminium alloys, have shown promise for various critical structural applications.

An important feature of the microstructure in the Al/SiC composites is the higher density of dislocations and larger residual internal stresses compared to the unreinforced alloys, which are introduced by the large difference in coefficients of thermal expansion between the reinforcement and matrix. The introduction of the reinforcement plays a key role in both the mechanical and thermal ageing behaviour of the matrix alloy, as well as the composite material. Micro-compositional changes, which occur during the thermo-mechanical forming processes of these materials, can cause substantial changes in mechanical properties such as ductility, fracture toughness and stress corrosion resistance.

An understanding of the work hardening behaviour of particulate reinforced metal matrix composites is crucial in optimising the parameters for deformation processing of these materials. The particulate composite material is not homogeneous; hence material properties not only are sensitive to the properties of the constituents, but also to the interfacial properties. The strength of particulate composites depends on the size of the particles, inter-particle spacing, and the volume fraction of the reinforcement [1].

In the case of particulate reinforced aluminium composites, the microstructure and mechanical properties can be altered by thermo-mechanical treatments as well as by changing the reinforcement volume fraction. The strengthening of a pure metal is carried out by alloying and supersaturating; to an extent, on suitable heat treatment, the excess alloying additions precipitate out (ageing). A study of the deformation behaviour of precipitate hardened alloy or particulate reinforced metal matrix composites shows that the interaction of dislocation with the reinforcing particles is much more dependent on the particle size, spacing and density than on the composition [2]. Furthermore, when a particle is introduced in a matrix, an additional barrier to the movement of dislocation is created and the dislocation must behave either by cutting through the particles or by taking a path around the obstacles [3].

At present, the relationship between the strength properties of metal matrix composites and the details of the thermo-mechanical forming processes is not well understood. The kinetics of precipitation in the solid state has been the subject of much attention. Early work of Zener on growth kinetics has been developed by Aaron and Aaronson [4] for the grain boundary case and by Aaron *et al.* [5] for intragranular precipitation. These approaches have been integrated to produce a unified description of the inter- and intra-granular nucleation and

growth mechanisms by Shercliff and Ashby [6] and Carolan and Faulkner [7]. More recently, successful attempts have been made to combine models of precipitate growth at interfaces with concurrently occurring segregation in aluminium alloys [8]. Studies of the relation between interfacial cohesive strength and structure have only recently become possible. This is due to of remarkable advances in physical examination techniques allowing direct viewing of interface structure and improved theoretical treatments of grain boundary structure.

The ability of the strengthening precipitates to support the matrix relies on the properties of the major alloying additions involved in the formation of these precipitates. The development of precipitates in Al-based alloys can be well characterised through heat treatment processing. Heat treatment affects the matrix properties and consequently the strain hardening of the composite. Furthermore, the distribution and concentration of these precipitates greatly affect the properties of the material where homogenous distribution of small precipitates provides the optimum results.

The role of the reinforcement is crucial in the microdeformation behaviour. The addition of SiC to aluminium alloy increases strength and results in high internal stresses, in addition to the ones caused by the strengthening precipitates. Furthermore, the SiC reinforced particles are not affected by the heat treatment process. A great deal of attention has been recently devoted to understanding the strengthening mechanisms in metal matrix composites, which are distinguished by a large particulate volume fraction and relatively large diameter. Another important matter in understanding and modelling the strength of particulate MMCs is to consider the effect of particle shape, size and clustering [9–11]. Lewandowski *et al.* [12] illustrated the important effects of clustering of reinforcement on the macroscopic behaviour as well as the effects of segregation to SiC/Al interfaces. Rozak *et al.* [13] presented the effects of casting condition and subsequent swaging on the microstructure, clustering, and properties of Al/SiC composites.

The purpose of this study is to define the features which significantly affect the microdeformation behaviour of a practical aluminium alloy/silicon carbide composite system, which are directly related to the forming processes currently being used by the industry.

2. MATERIALS

The metal matrix composites studied were aluminium–silicon–magnesium alloy matrix (A359) reinforced with varying amounts of silicon carbide particles. Aluminium alloys A359 are important materials in many industrial applications, including aerospace and automotive applications.

For the investigation, four types of material were used: (1) ingot as received 359/40% SiC, with an average particle size of 19 ± 1 micron, (2) ingot as received A359/25% SiC, with an average particle size of 17 ± 1 micron, (3) hot rolled as received A359/31%SiC with an average particle size of 17 ± 1 micron and (4) cast

alloy as received A359/30% SiC with particles of F400grit, with an average particle sizes of 17 ± 1 micron. Table 1 contains the details of the chemical composition of the matrix alloy as well as the amount of silicon carbide particles in the metal matrix composites according to the manufacturer [14]. The alloys from the Al–Si–Mg system are the most widely used in the foundry industry because of their good castability and high strength-to-weight ratio.

The microstructure of such materials consists of a major phase, aluminium or silicon and the eutectic mixture of these two elements. In this system, each element plays a role in the material's overall behaviour. In particular, Si improves the fluidity of Al and also Si particles are hard and improve the wear resistance of Al. By adding Mg, Al–Si alloy becomes age hardenable through the precipitation of Mg_2Si particulates. One can refer to an article by Strangwood *et al.* that quantifies the segregation to SiC/Al interfaces using TEM and *in situ* analyses to show Mg segregation to interfaces [15].

An additional advantage of Al–Si alloys for casting applications is that Si expands on solidification. Silicon and magnesium are often added in balance to form the quasi-binary Al–Mg_2Si, although sometimes Si is added in excess of that needed to form Mg_2Si. The phase diagram of the Al–Si system in Fig. 1 [16] shows

Table 1.
Chemical composition (wt%) (MC-21)

Types	Si	Mg	Mn	Cu	Fe	Zn	SiC
Ingot A359	9.5	0.5	0.1	0.2	0.2	0.1	40
Ingot A359	9.5	0.5	0.1	0.2	0.2	0.1	25
Cast A359	9.5	0.5	0.1	0.2	0.2	0.1	30
Rolled A359	9.5	0.5	0.1	0.2	0.2	0.1	31

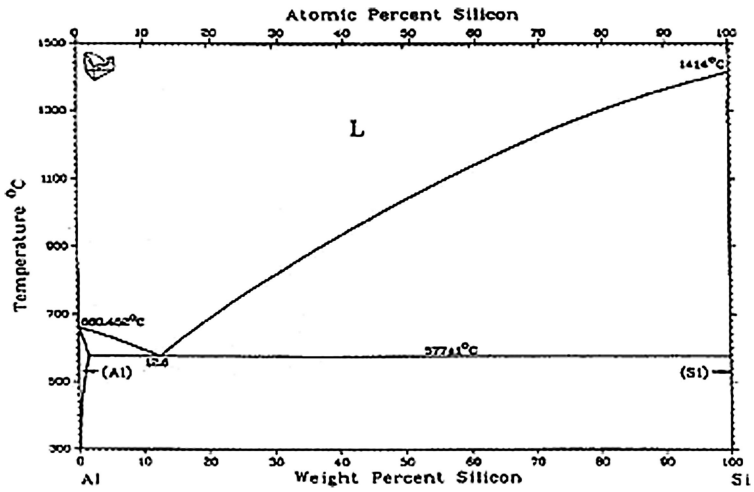

Figure 1. Al–Si phase diagram [10].

(a) (b)

Figure 2. MC-21 MMC fabrication setup. (a) MMC mixer and (b) MMC holding furnace.

a eutectic with some solubility of Si in Al, but negligible solubility of Al in Si. The precipitation sequence is supersaturated solid solution $\rightarrow$ GP zones $\rightarrow$ $\beta' \rightarrow \beta$ (Mg_2Si). The GP zones are needled-shaped along the aluminium matrix and the β' phase is rod-shaped along the matrix. The equilibrium phase β is face centered cubic and forms platelets on the matrix [17].

The materials used were kindly supplied by MC-21, Inc located in Carson City, NV, USA, which developed, patented, and demonstrated at commercial scale a proprietary process improvement that achieves much greater efficiency in the mixing operation (Fig. 2(a) and 2(b)). This increased efficiency allows SiC particles to be mixed into molten aluminium much more rapidly. In addition, lower cost SiC particles possessing wider size distributions could be used and higher amounts of SiC particles included into the molten mixture: up to 45 vol% SiC could be achieved [14].

The benefits of the rapid mixing process developed by MC-21, Inc. include its demonstrated ability to produce a much wider range of reinforcement size and volume fraction combinations. For example, materials with twice the stiffness of aluminium at comparable density greatly reduced thermal expansion coefficient and orders of magnitude improvement in wear resistance are achievable in the higher reinforcement volume fraction composites.

3. HEAT TREATMENT

Properties in particulate metal matrix composites are primarily dictated by the uniformity of the second-phase dispersion in the matrix. The distribution is controlled by solidification and can be later modified during secondary processing. In particular, due to the addition of magnesium in A359, the mechanical properties of this alloy can be greatly improved by a heat treatment process. There are many

different heat treatment sequences and each one can modify the microstructural behaviour as desired [11].

One of the most used — T6 heat treatment — consists of the following steps: solution heat treatment, quenching and age hardening. In the solution heat treatment, the alloy is heated to a temperature just below the initial melting point of the alloy, where all the solute atoms are allowed to dissolve to form a single phase solid solution. The alloy is then quenched to room temperature at a rate sufficient to inhibit the formation of Mg–Si precipitates, resulting in a non-equilibrium solid solution that is supersaturated. In age hardening, the alloy is heated to an intermediate temperature where nucleation and growth of the Mg–Si precipitates can occur. The precipitate phase nucleates within grains and at grain boundaries, as uniformly dispersed particles. The holding time plays the key role in promoting precipitation and growth which results in higher mechanical deformation response of the composite. The material is then cooled to room temperature, where it may receive further processing.

There is another aspect that needs to be considered in the heat treatment of composites, which is that the particles introduced may alter the alloys surface characteristics and increase the surface energies. The process variables affecting the dispersion of the particulate is very important, including temperature and time of heat treatment of the particles, particle size and shape, melt temperature at the introduction of the particulate, feed rate of the particulate, volume percent of the dispersoid and melt degassing.

The factors influencing the type and form of reinforcement used are the desired material properties, ease of processing and part fabrication. In the early stages of development, only a limited range of reinforcements could be used. The stability between the components and the differences in their thermal properties, such as coefficient of thermal expansion and coefficient of thermal conductivity, are the limiting factors in the compatibility of the two materials used to make the composite [18].

A good bond can be formed by proper and adequate interaction between the reinforcement and the matrix. Inadequate interaction results in lack of proper bonding, whereas excessive interaction leads to the loss of the desired properties and inferior performance of the MMC. The thermal conditions for this reaction depend on the composition of the MMC and its processing method. As the reaction progresses, the activity of silicon in liquid aluminium increases and the reaction tends to saturate. The presence of free silicon in an aluminium alloy has been shown to inhibit the formation of Al_4C_3. Temperature control is extremely important during the fabrication process. If the melt temperature of SiC/Al composite materials rises above a critical value, Al_4C_3 is formed, increasing the viscosity of the molten material, which can result in severe loss of corrosion resistance and degradation of mechanical properties in the cast composite; excessive formation of Al_4C_3 make the melt unsuitable for casting.

It is known that molten aluminium does not wet silicon carbide readily, which is one of the major concerns that needs to be overcome to prevent silicon carbide particles being displaced from molten aluminium and to ensure SiC/Al bonding. In addition, as mentioned, heating above a critical temperature can lead to the undesirable formation of Al_4C_3 flakes. MC-21, Inc. patented melt stirring, a method of satisfying these requirements and producing high quality composites. SiC particulates are added to Al–Si casting alloys, where Si in the alloy slows down the formation of Al_4C_3. The process yields material with a uniform distribution of particles in a 95–98% dense aluminium matrix. The rapid solidification, inherent in the process, ensures minimal reaction between reinforcing material and the matrix [14].

4. METALLOGRAPHIC EXAMINATION AND MICRO-HARDNESS TESTING

In order to analyse the microstructure, a series of sample preparation exercises were carried out, consisted of the cutting, mounting, grinding and polishing of the samples. The microstructures were investigated by using an optical microscope Leica DM 4000M, image analysis software, a Philips XL40 Scanning Electron Microscope with a link 860 EDAX, a Philips FEI Nova Nano-Scanning Electron Microscope, a Philips X-ray fluorescence spectrometer (XRF) and X-ray diffraction (XRD) techniques with a link to Philips X'Pert High Scores software 2000. The microhardness was determined by a Mitutoyo Muk-H1 Hardness tester.

In particular, Struers Accutom-5 was used to cut the specimens to the desired size; a Struers SpeciFix-20, epoxy cold mounting system was used to mount the specimens in order to prevent thermal damage of the mounting specimen; and a Struers RotoPol-25 grinding machine was used for the grinding and polishing operations. The grinding was performed with Struers Silicon Carbide grinding papers with water lubrication. This grinding was done manually and light pressure was applied. This was followed by polishing, using the DP-Dac polishing cloth with DialPro Dac stable diamond suspension containing a mixture of diamonds and cooling lubricant with 6, 3 and 1 μm particulate size. Furthermore, colloidal silica was used for the final polishing to ensure an optimum surface.

The microstructures were investigated by SEM, EDAX XRD and image analysis pro software, to determine the Al/SiC area percentage, size and count of particulates. The area percentage of SiC was measured as the area of a particular microstructure image, divided by the area of the SiC represented in that image, by using the autobeam feature of the SEM microscope (Fig. 3). The results show that area percentage of Al, SiC and Si satisfies the manufacturers' data. Also, magnesium as well as a small percentage of oxygen was identified. Apart from the major elements, traces of Fe, Mn, Zn, and Cu were also identified (Fig. 4(a)). By using EDAX technique and quantitative analysis, percentages of the alloying elements were also obtained and found similar to the XRF elemental analysis percentages in weight percentage and close to the manufacturers' values. (Fig. 4(b); Table 2).

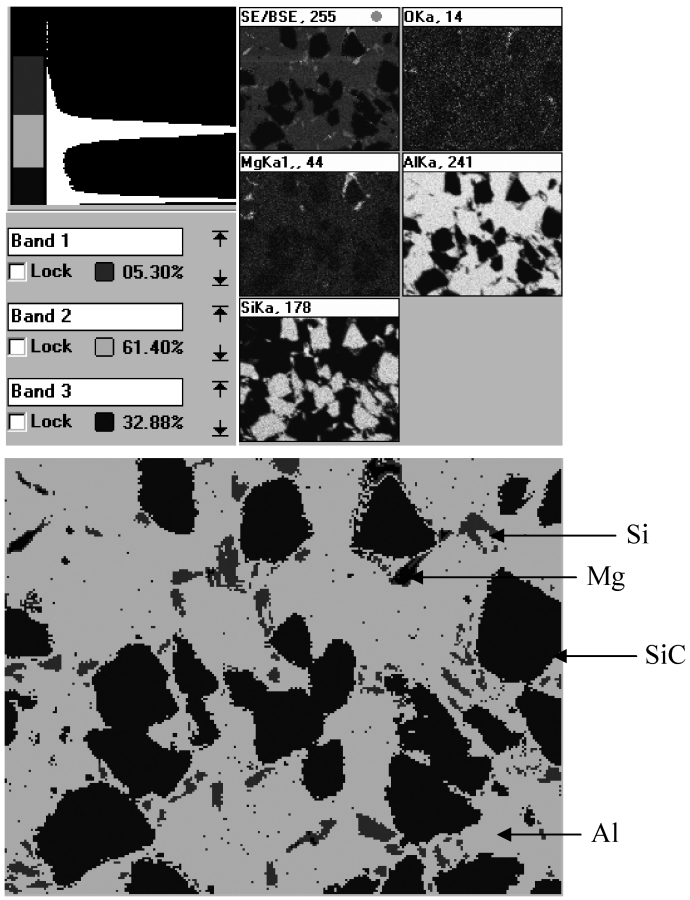

Figure 3. SEM mapping analysis of Cast A359/30%SiC microstructure showing four distinct phases — Al, SiC, silicon and magnesium.

The microstructures of the examined MMCs have four distinct micro phases, (as marked) which are as follows: the aluminium matrix (grey area), the SiC particles (dark area), the eutectic region of aluminium and silicon (white area and grey area) and the Mg_2Si phase (white area) (Fig. 5(a) and 5(b)). The SiC particles were found to lie in the eutectic region. This is because, in MMCs, the SiC particles tend to aggregate in the eutectic region at the end of the solidification process. The distribution of SiC particles was found to be more or less uniform; however, instances of particle free zones and particle clustered zones were found. A typical microstructure of the metal matrix composite is shown in Fig. 6.

The X-ray diffraction was carried out on the MMCs with 25%, 30%, 31% and 40% of SiC particulates. Even though some peaks were superimposed, the results showed the phases present in the microstructures. In particular, the results showed existence of aluminium matrix, eutectic silicon, SiC, Mg_2Si, SiO_2 phases as the distinct ones, and also $MgAl_2O_4$, Al_2O_3 phases, that do superimpose with other

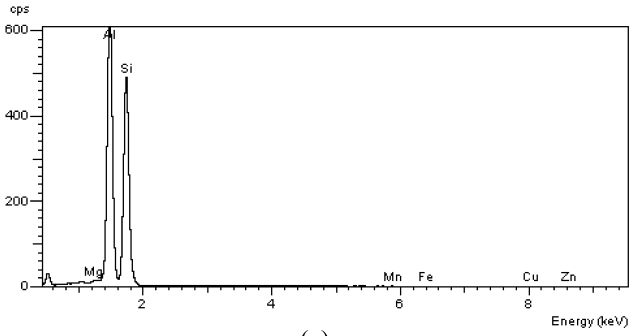

(a)

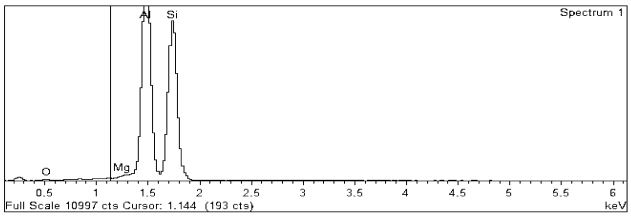

Label	Range (keV)	Gross	Net	% total
OKa	0.447 to 0.608	5330	1159	0.2
MgKa1,	1.168 to 1.347	17017	907	0.2
AlKa	1.388 to 1.587	415786	368712	66.1
SiKa	1.648 to 1.847	219629	187152	33.5

(b)

Figure 4. (a) Hot-rolled A359/31% SiC-EDAX Analysis showing traces of Mn, Fe, Cu and Zn identified and (b) EDAX-Ingot A359/25% SiC elemental quantitative analysis showing percentage of Al, Si, Mg and oxygen elements present.

Table 2.
XRF elemental analysis of hot rolled and cast samples

Element MMC	Mass % (weight)	
	Hot rolled A359/31% SiC	Cast A359/30% SiC
Al	56.08	61.43
Si	42.03	37.20
Mg	0.533	0.424
Fe	0.437	0.387

major phases but they have been accepted as possibilities (Fig. 7(a)–7(c)). In addition, the presence of $MgAl_2O_4$ shows that magnesium reacted with SiO_2 at the surface of SiC and formed this layer in the interfacial region between the matrix and the reinforcement. The layers of $MgAl_2O_4$ protect the SiC particles from the liquid aluminium during production or remelting of the composites. This layer provides more than twice the bonding strength compared to Al_4C_3. The presence of Al_4C_3 could not be identified by XRD, something that verifies that high percentage of

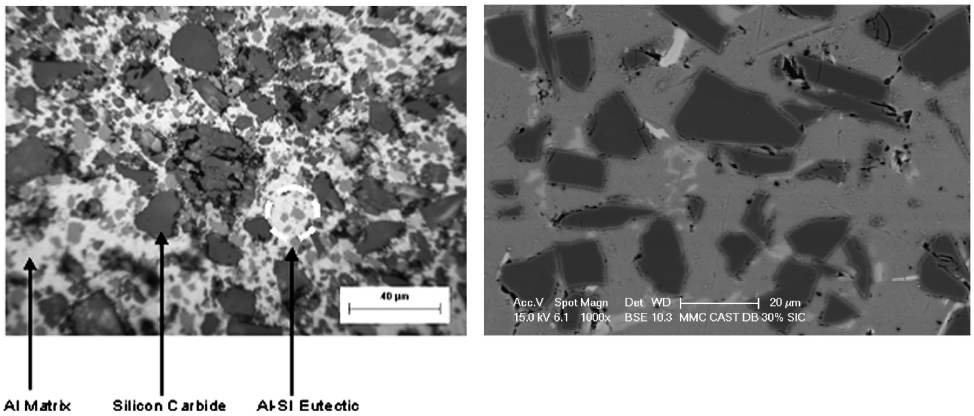

Figure 5. (a) Hot-rolled A359/31%SiC showing microstructure distinct phases and (b) Cast A359/30% SiC showing phases. Dark objects-SiC, Grey area-Al, Light white area-Si, white area-Mg.

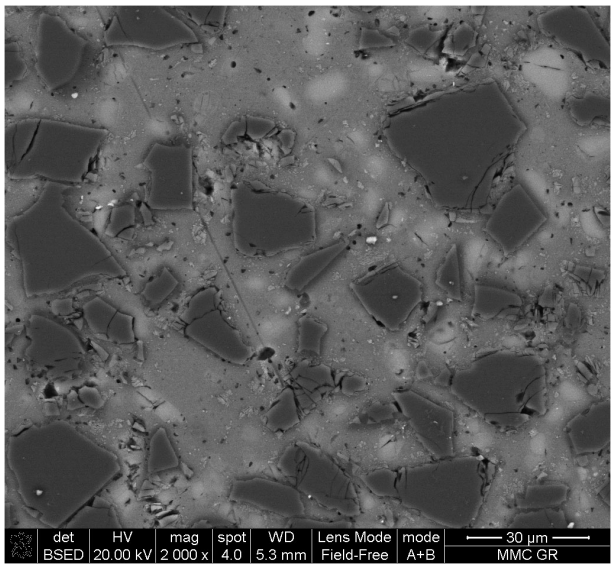

Figure 6. Microstructure of MMC-hot rolled A359/31% SiC showing reinforcement homogeneous distribution and phases as well as porosity.

Si added in the composite during manufacturing and also the existence of Al_2O_3 retards Al_4C_3 formation in the composite [19].

Interfaces of the matrix/reinforcement were identified by using a high magnification Nano-SEM microscope. In the hot rolled images, interfaces of Al matrix/SiC reinforcement are clearly shown, and also Si phase area is identified close to the interface creating an Al–Si interphase (Fig. 8(a)). This interphase attains properties coming from both individual phases and facilitates the strengthening behaviour of

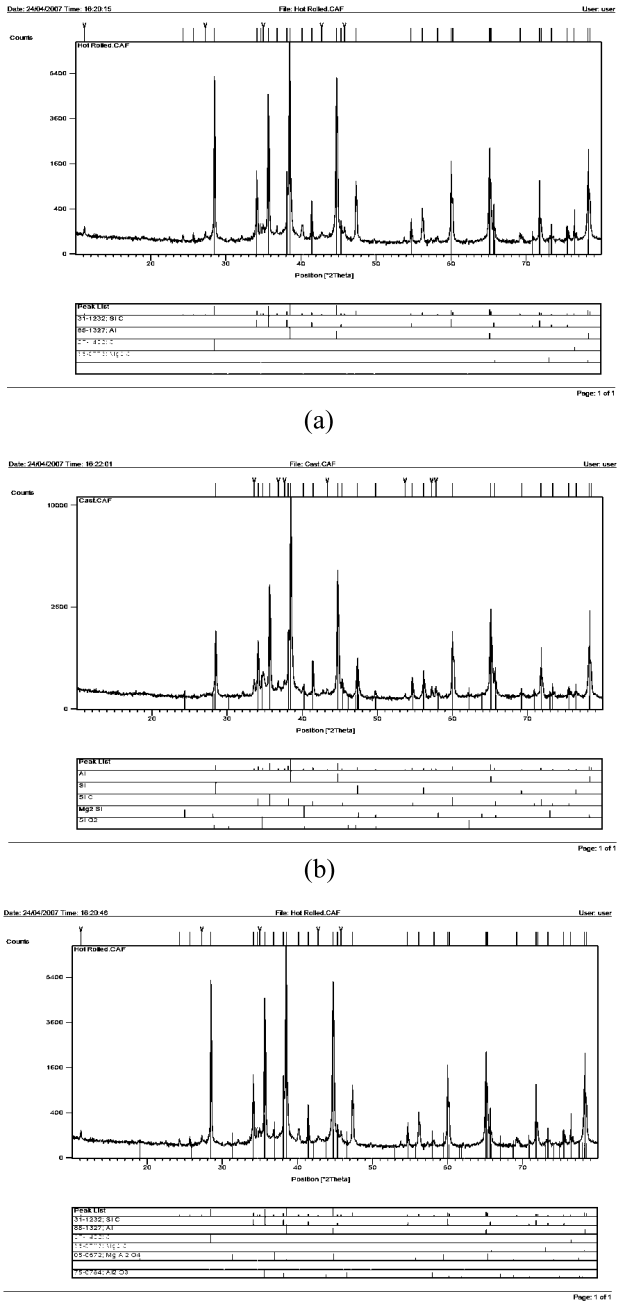

(a)

(b)

(c)

Figure 7. (a) Hot-rolled A359/31% SiC-XRD analysis, (b) Cast A359/30% SiC-XRD analysis and (c) Cast A359/30% SiC-XRD analysis, showing definite phases as well as two possible superimposed ones.

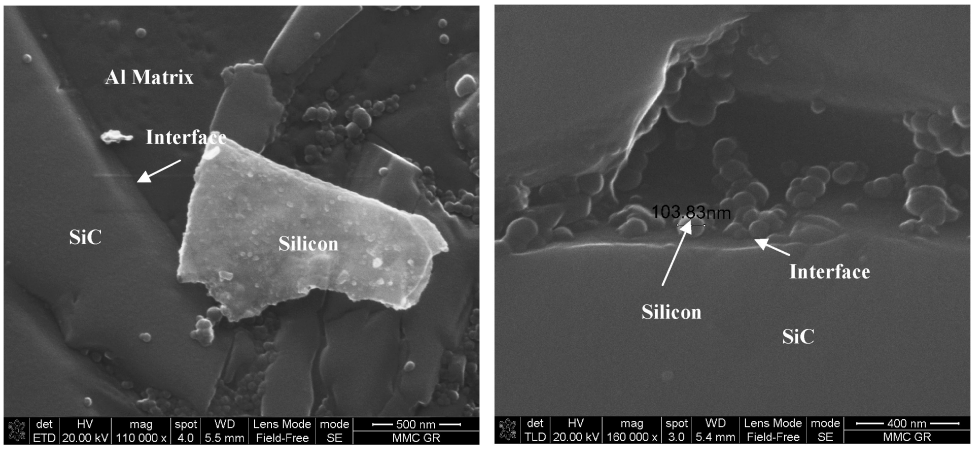

(a) (b)

Figure 8. (a) Hot-rolled A359/31% SiC showing interface and (b) nano-SEM image of Al–SiC interface. Round particles measuring 103.83 nm are silicon.

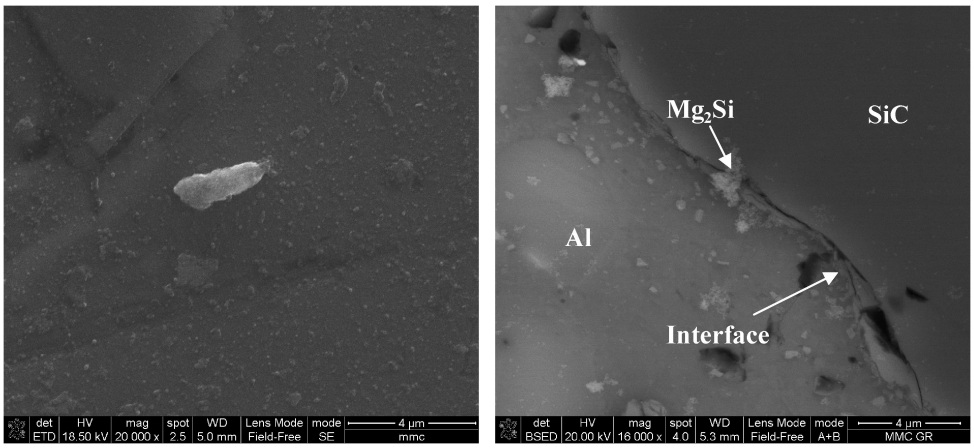

(a) (b)

Figure 9. (a) Mg_2Si precipitate formed close to interface and (b) hot-rolled A359/31% SiC showing interface of Al/SiC and also small precipitates of Mg_2Si (white areas close to the interface).

the matrix/reinforcement interface. Furthermore, silicon particles can be identified in round form close to the interface of Al/SiC in a size of approximately 100 nm (Fig. 8(b)). These silicons could form the SiO_2 layer when magnesium and oxygen are present and this will lead to the formation of $MgAl_2O_4$ phase.

Moreover, objects in a random shape have been identified and after EDAX and mapping techniques, it was observed that these objects formed of many round particles stacked together, which may well be Mg_2Si precipitates, bearing in mind that the presence of Mg and Si was identified in the earlier study [8] (Fig. 9(a) and 9(b)).

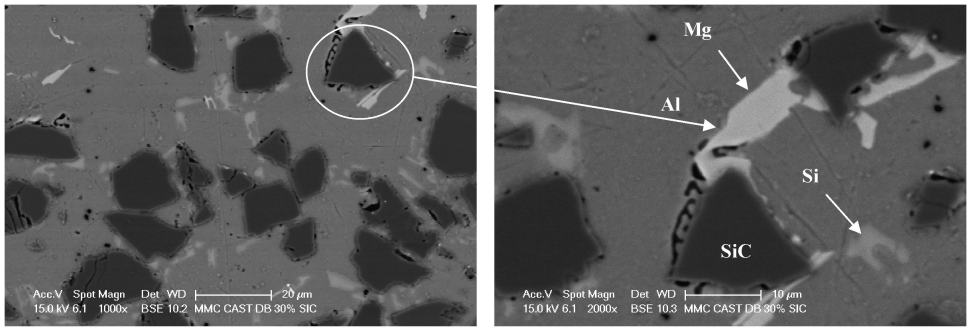

(a) (b)

Figure 10. (a) Microstructure of Cast A359/30% SiC and (b) microstructure of Cast A359/30% SiC showing four distinct phases.

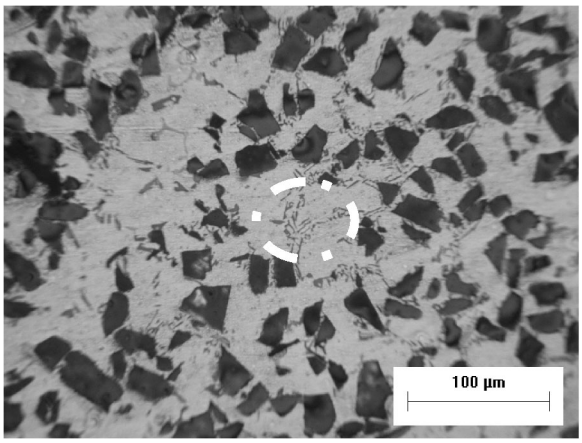

Figure 11. Ingot A359/25% SiC, showing dendritic Al–Si arms and homogeneous distribution of SiC reinforcement.

In the cast sample, a homogenous distribution of the SiC and also the three distinct phases has been observed. Also, the microstructure of this composite clearly shows that the magnesium phase lay next to the reinforcement and, because Si was present, precipitation is possible (Fig. 10(a) and 10(b)). In the ingot samples, the matrix Al-alloy shows the classic dendritic microstructure of Al–Si containing silicon particles (Fig. 11). The composite as a whole though shows that the reinforced SiC particles distribute rather homogeneously along the interdendritic arms. Furthermore, it is noted that Si nucleates and grows on SiC particles and in many cases, a considerable number of SiC particles are joined together by the Si phase (Fig. 8(b)).

From the images, it can be seen that uniform distribution of the reinforcements in all materials examined was achieved, and shrinkage and porosities were observed in the samples. A total avoidance of porosity is difficult, because the lower thermal conductivity of ceramic reinforcements requires them to be pushed to the solidifying front of a freezing melt, in such a way that shrinkage porosities appear around

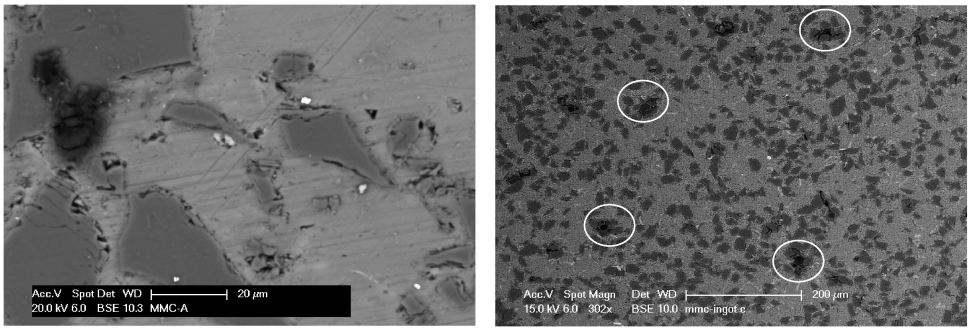

(a) (b)

Figure 12. (a) Ingot A359/25% SiC showing porosity of 10 ± 5 μm and (b) ingot A359/40% SiC showing porosity of 10 ± 5 μm.

the particulate, as the matrix shrinks during solidification. Also, as magnesium is surface active, it effectively reduces interfacial energies, only with an optimum amount of reinforcements; otherwise, both gas (due to air) and shrinkage porosities will result [20].

Microscopic porosity was observed in specific areas of the reinforced and unreinforced regions of the composites. Porosities of 10 ± 5 μm in size and ≈ 1 wt% were present in the materials examined: some in the particle free region at very close proximities to the free surface and some found closer to the SiC particles (Fig. 12(a) and 12(b)). These areas consist of a thin skin that has solidified before the rest of the unreinforced region due to cooling by air convection and heat irradiation. As a result, most of these porosities have been formed by solidification shrinkage, as is evident by their irregular shapes. Such porosities represent no major problem for application purposes, since this skin can be machined away.

In addition, during machining and cutting of the composite and due to the high hardness of the reinforcement, it is likely to have partial debonding of the particles creating voids and pit holes.

In order to compare the four samples in relation to the reinforcement percentage and also the different manufacturing forming process, a microhardness test was performed. The microhardness test method, according to ASTM E-384, specifies a range of loads using a diamond indenter to make an indentation, which is measured and converted to a hardness value [21]. Microhardness of the four composites has been measured in order to get the resistance of the material to indentation, under localized loading conditions.

Measuring the different phases in the micro-level is quite challenging, as SiC reinforcement of ≈ 17 μm of size was not easy to measure, due to the small indentation mark left when a small load is used on the carbide. When higher values of load were introduced, the indentation was not localized in the carbide but covered some of the matrix area. The load after test and trial technique was set to 50 g where

Table 3.
Microhardness Vickers (Hv) testing results in Al/SiC composites

	Hv0.05			Mean	
Ingot A359/40% SiC					
Al matrix	108.5	120.8	114.4	115	–
Sic	2178	2360	2213	2250	–
MMC	205	211	255	224	–
Ingot A359/25% SiC					
Al matrix	94.9	100.7	92.6	96	↓
Sic	2480	2530	2470	2493	↑
MMC	207.1	200.3	202.1	203	↓
Cast A359/30% SiC/F360					
Al matrix	100.6	97.6	93.5	97	↑
Sic	2610	2453	2315	2459	↓
MMC	200.5	172	195	189	↓
Rolled A359/31% SiC					
Al matrix	86.2	79.1	70.2	79	↓
Sic	2162	2242	2454	2286	↓
MMC	167.3	145.5	137.8	150	↓

SiC, aluminium matrix as well as the overall composite (MMC) was measured to give the values of the microhardness.

The microhardness values of the aluminium matrix reinforced with higher volume fraction showed higher values than the aluminium matrix reinforced with lower volume fraction (Table 3). The difference of the Al matrix readings compared with the SiC ones is excessive and this results in having an inhomogeneous plastic deformation of the ductile aluminium matrix and the brittle SiC particles.

Furthermore, readings for the ingot samples, and particularly for the 40% SiC sample with the higher measured particulates values, showed better hardness than the cast sample, whereas the hot rolled sample showed the lowest values in the matrix as well as in the overall composite readings (Fig. 13(a)–13(c)). The latter statement leads to the conclusion that reinforcement percentage, interparticle spacing and also particle size play a key role in microhardness values. Finally, manufacturing forming processes influences materials' microhardness behaviour in relation to the reinforcement percentages of the composites.

5. MODEL

A method of calculation has been applied to predict the interfacial fracture strength of aluminium, in the presence of magnesium segregation. The model shows success in making prediction possible of trends in relation to segregation and intergranular fracture strength behaviour in metallic alloys [8]. Small changes in surface energy

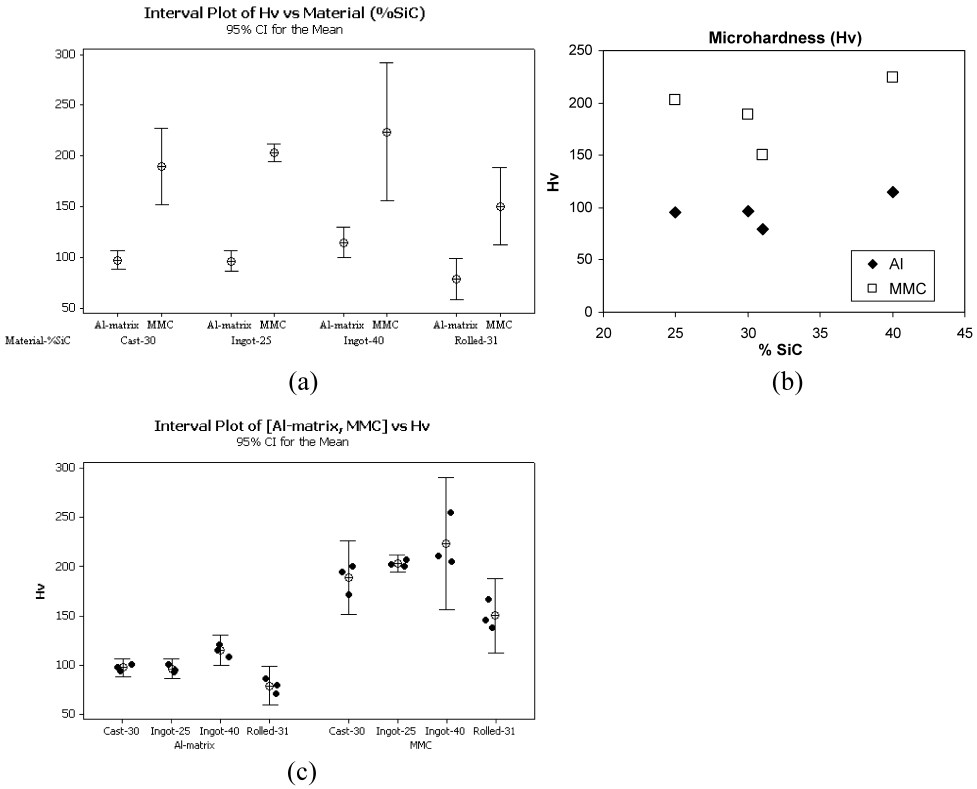

Figure 13. (a) Microhardness values measured (with predicted range) showing ingot samples having higher values in both matrix and overall MMC, (b) microhardness values measured showing percentage of SiC related values. Higher percentage of SiC gives higher values except in the hot rolled sample where due to the processing values drop and (c) microhardness values measured showing readings for aluminium and overall MMC materials. MMC readings are higher than Al-matrix.

caused by segregation will result in very large changes in intergranular fracture stress.

The interface structure is important in determining the amount of predicted segregation and hence the change of the interfacial energy caused by the segregation. Equations have been developed to forecast the energy change in terms of the coincidence site stress (σ_α) value describing the boundary, and the formation energies of impurities on the boundary. The model indicates that low angle boundaries and those with low σ coincidence site values will be less susceptible to fracture than high angle boundaries. The work of intergranular fracture is G_k given by,

$$G_\mathrm{k} = A\sigma_\mathrm{p} \mathrm{e}^{n \ln(\sigma/\sigma_\mathrm{o})}, \tag{1}$$

where A is the dislocation pile-up term describing the effectiveness of dislocations in providing stress concentration at the advancing intergranular crack tip (=100), n is the strain rate hardening exponent, σ_p is the energy involved with creating the

fracture surface with

$$\sigma_p = 2\sigma_s - \sigma_{gb}(= \sigma_o),$$

σ_s is the surface energy, σ_{gb} is the grain boundary energy, and σ_a is the new interfacial energy caused by segregation, given by,

$$\sigma_a = \sigma_o - ZRT \ln(1 - c + Bc), \tag{2}$$

where Z is the term describing the density of interface sites which are disordered enough to act as segregation sites, R is the gas constant, also known as the universal molar gas constant, is a physical constant that appears in an equation defining the behaviour of a gas under theoretically ideal conditions. The gas constant is, by convention, given the value $R = 0.286$ kJ/kg/K, T is the absolute temperature, c is the segregate concentration needed to cause embrittlement (=0.1), B is a term describing the modification of the boundary energy by impurities using the Zuchovitsky equations, given by;

$$B = e^{\sigma_{gb}/Z + H_v/2kT}, \tag{3}$$

where H_v is the enthalpy of formation of the impurity atom in the bulk (in e.V), k is Boltzmann's constant, Z is assumed constant for all boundaries in equation (3).

In the non-equilibrium segregation mechanism, by altering the heat treatment process the effects of second phase particles/reinforcement will change and the desired intergranular fracture strength can be achieved. If the segregation is equilibrium, other more strongly segregating elements may be introduced in order to attain the desired outcomes.

The model shows success in making prediction possible of trends in relation to segregation and precipitation behaviour in metallic solids. Further work is in progress to give a more quantitative forecast of the effects of second phase particles/reinforcement on mechanical properties of matrix-reinforcement interface in metal matrix composites.

6. DISCUSSION

Microstructure analysis of aluminium SiC composites shows the deformation that takes place in the material. Phase deformations in the hot-rolled samples create the Al–Si phase but Mg reaction produces Mg_2Si precipitates, following the appropriate heat treatment. In the ingot samples, the dendritic microstructures of Al–Si clearly satisfy the process of homogenisation due to the nature of equilibrium segregation. Moreover, the general distribution and the size of the SiC particulates were satisfactory.

In addition, the porosity observed shows that the material has some kind of imperfection in the 'as-received' condition, something that may change by artificial ageing. In general, the porous percentage is low and the material cannot be considered as defective.

Furthermore, the importance of the volume fraction of the precipitates and the reinforcement, as vital factors, needs to be focused upon. Dispersion of the particles, their mean size and the typical distance between them affects the microdeformation behaviour. Interaction mechanisms between particles and dislocations of precipitated particles can effectively impede the motion of dislocations in the matrix. If the particle is coherent with the matrix, i.e. if the glide planes of the matrix continue through the particle, a dislocation can intersect the particle.

From the microhardness testing it can be noticed that the percentage of reinforcement phase plays a crucial role in the overall composite hardness behaviour. Also, while segregation was identified as the principal strengthening mechanism of interfaces in SiC-particulate reinforced aluminium matrix composites, other features also contribute to a lesser extent to the measured increase of microhardness near the interface compared to Al matrix. Such features are:

(a) Local chemistry changes due to Mg segregation and formation of spinel ($MgAl_2O_4$);

(b) Constraint effects provided by the SiC particles, which is harder than the deforming matrix;

(c) Potentially higher dislocation density near the SiC particles due to mismatch in the coefficient of thermal expansion; and

(d) Residual stresses near SiC particles due to mismatch in the coefficient of thermal expansion.

Moreover, with increasing volume fraction, the number of particles increases, whereas spacing between particles decreases. Consequent increase in the number of barriers to plastic deformation reduces the depth of plastic deformation by restraining the plastic flow of the matrix. This can lead to low fracture toughness of the composite, which has to be avoided. Lower percentage shown in the hot rolled samples may be ideal as ductility of the matrix with a low percentage of SiC lead to the best composite behaviour, in relation to the application for the composite to be used. More work has to be done regarding the percentage of the phases in the material, in relation to mechanical behaviour.

To achieve good mechanical properties, a good globular microstructure must be obtained with very fine and homogeneous SiC distribution and with very low levels of voids produced during the solidification process. By using heat treatments, the mechanical properties of such materials can be strongly improved. Tensile tests and fracture toughness K_{1C} tests of the material can be performed in the as-received and as heat-treated conditions, in order to observe the different fracture behaviour as a result of different heat treatments cycles. An objective is to observe whether or not, in the monotonic tensile testing, reinforcement with SiC particulates produces a substantial increase in the work hardening of the material. This increase can be related to a more significant manner with increasing volume fraction of carbides. Also, from the fracture toughness value, an understanding of the macroscopic

behaviour of the material during fracture studies can be observed and related with the microscopic prediction of the interfacial fracture strength.

Furthermore, investigation of the yield and ultimate tensile strength and the elastic modulus of the material need to be undertaken. The relationship of the microscopic and the macroscopic interfacial strength behaviour of the MMC will be the final objective to be investigated.

7. CONCLUSIONS

The micro-structural events of segregation and precipitation in metal matrix composites have been investigated, at the micro-level, and the developments of local concentration gradients around the reinforcement have been identified. A method of calculation identifies the role played by Si and Mg segregants on the interfacial strengthening of a metal-ceramic interface.

We propose a method of nano-scale phase identification and matrix-reinforcement/micro-hardness measurement, which has proven to be successful in this work. Microhardness testing showed a significant difference in values of hardness of the Al-matrix and SiC reinforcement in favour of SiC, whereas readings coming from areas close to the matrix and reinforcement (interphase areas) showed increase of the hardness of the material. The interparticle distance, the mean sizes of the particulates, as well as their percentage, in the composite are the major factors affecting this microhardness variability.

Acknowledgements

Support of this work by MC-21 Inc, and in particular Dr. David Schuster, is gratefully acknowledged. Also, many thanks to Dr. Georgios Chliveros for useful discussions and to Mr. Leon Bowen, for his valuable technical assistance and for many useful discussions throughout the length of this experimental study.

REFERENCES

1. L. J. Broutman, R. H. Krock and K. G. Kreider, Composite materials, in: *Metallic Matrix Composites*, K. G. Kreider (Ed.), Vol. 4. Academic Press, New York and London (1974).
2. D. J. Lloyd, Particle reinforced aluminium and magnesium matrix composites, *Int. Mater. Rev.* **39**, 1–23 (1994).
3. N. F. Mott and F. R. N. Nabarro, An attempt to estimate the degree of precipitation hardening, with a simple model, *Proc. Phys. Soc.* **52**, 85 (1940).
4. H. B. Aaron and H. I. Aaronson, Growth of grain boundary precipitates in Al-4% Cu by interfacial diffusion, *Acta Meter.* **16**, 789 (1968).
5. H. B. Aaron, D. Fainstein and G. R. Kotler, Diffusion-limited phase transformations: a comparison and critical evaluation of the mathematical approximations, *J. Appl. Phys.* **41**, 4404–4410 (1970).
6. H. R. Shercliff and M. F. Ashby, A process model for age hardening of aluminium alloys — I. The model, *Acta Mater.* **38**, 1789–1802 (1990).

7. R. A. Carolan and R. G. Faulkner, Grain boundary precipitation of $M_{23}C_6$ in an austenitic steel, *Acta Mater.* **36**, 257–266 (1988).
8. S. T. Hasan, J. H. Beynon and R. G. Faulkner, Role of segregation and precipitates on interfacial strengthening mechanisms in SiC reinforced aluminium alloy when subjected to thermomechanical processing, *J. Mater. Process. Technol.* **153–154**, 757–763 (2004).
9. M. Manoharan and J. J. Lewandowski, *In situ* deformation studies of an aluminum metal–matrix composite in a scanning electron microscope, *Scr. Metall.* **23**, 1801–1804 (1989).
10. M. Manoharan and J. J. Lewandowski, Effect of reinforcement size and matrix microstructure on the fracture properties of an aluminum metal–matrix composite, *Mater. Sci. Eng. A* **150**, 179–186 (1992).
11. S. T. Hasan, Effect of heat treatment on interfacial strengthening mechanisms of second phase particulate reinforced aluminium alloy, *14th Int. Metall. Mater. Conf. (Metal 2005)*, Hradec nad Moravici, Czech Republic (2005).
12. J. J. Lewandowski, C. Liu and W. H. Hunt, Jr., Effects of microstructure and particle clustering on fracture of an aluminum metal matrix composite, *Mater. Sci. Eng. A* **107**, 241–255 (1989).
13. G. Rozak, J. J. Lewandowski, J. F. Wallace and A. Altmisoglu, Effects of casting conditions and deformation processing on A356 aluminum and A356-20% SiC composites, *J. Compos. Mater.* **26**, 2076–2106 (1992).
14. MC-21, Inc, Carson City, NV, USA, Technical Report. Available at www.mc21inc.com
15. M. Strangwood, C. A. Hippsley and J. J. Lewandowski, Segregation to SiC/Al interfaces in Al based metal matrix composites, *Scr. Metall.* **24**, 1483–1488 (1990).
16. T. B. Massalski, Binary alloy phase diagrams. ASM International, Metals Park (1986).
17. A. K. Vasudevan and R. D. Doherty, *Aluminum Alloys — Contemporary Research and Applications*. Academic Press, London, UK (1989).
18. Y. Li and K. T. Ramesh, Influence of particle volume fraction, shape and aspect ratio on the behaviour of particle-reinforced metal–matrix composites at high rates of strain, *Acta Mater.* **46**, 5633–5646 (1998).
19. U. Cocen, K. Onel and I. Ozdemir, Microstructures and age hardenability of Al-5%Si–0.2%Mg based composites reinforced with particulate SiC, *Compos. Sci. Technol.* **57**, 801–808 (1997).
20. G. Ramani, R. M. Pillai, B. Pai and K. G. Satyanarayana, Effect of dispersoid loading on porosity and Mg distribution in 6061–3% Mg–SiC_p composites, *Acta Mater.* **73**, 405–410 (1993).
21. Annual Book of ASTM Standards, Standard test method for microindentation hardness of materials, E384-99 (2005).